Introducing pseudo-capacitive bioelectrodes into a biofuel cell / biosupercapacitor hybrid device for optimized open circuit voltage

Sabine Alsaoub, Felipe Conzuelo, Sébastien Gounel, Nicolas Mano, Wolfgang Schuhmann, Adrian Ruff

Introducing pseudo-capacitive bioelectrodes into a biofuel cell / biosupercapacitor hybrid device for optimized open circuit voltage

Sabine Alsaoub[a], Felipe Conzuelo[a], Sébastien Gounel[b,c], Nicolas Mano[b,c], Wolfgang Schuhmann*[a], Adrian Ruff*[a]

Abstract: We report the fabrication of a polymer/enzyme based biosupercapacitor (BSC)/biofuel cell (BFC) hybrid device with optimized cell voltage that can be switched on demand from energy conversion to energy storage mode. The redox polymer matrices used for the immobilization of the biocatalyst at the bioanode and biocathode act simultaneously as electron relays between the integrated redox enzymes and the electrode surface (BFC) and as pseudo-capacitive charge storing elements (BSC). Moreover, due to the self-charging effect based on the continuously proceeding enzymatic reaction, a Nernstian-shift in the pseudo-capacitive elements, i.e. in the redox polymers, at the individual bioelectrodes leads to a maximized open circuit voltage of the device in both operating modes. Comparison with a conventional fuel cell design, i.e. using redox mediators with redox potentials that are close to the potentials of the used redox proteins, indicates that the novel hybrid device shows a similar voltage output. Moreover, our results demonstrate that the conventional design criteria commonly used for the development of redox polymers for the use in biofuel cells have to be extended by considering the effect of a Nernstian-shift towards the potentials of the used biocatalysts in those pseudo-capacitive elements.

Introduction

Biofuel cells (BFCs) are *energy conversion* devices in which enzymes or microbial systems are used as bioelectrocatalysts that convert chemical energy (stored in chemical bonds) into electrical energy (electrons) by continuously oxidizing a fuel at the anode and reducing an oxidant at the cathode (steady state operation mode) [1–3]. In recent years, biosupercapacitors (BSCs) were presented as a new type of *energy storage* devices in which the chemical energy is first transferred into a charge storage matrix by means of the biocatalyst, before it is finally released on demand within a short burst in form of a pronounced current spike (pulsed operation mode).[4,5]

For both devices, redox polymers[6] proved to be suitable immobilization matrixes for the active biocatalyst (for recent examples on redox polymer-based BFCs and BSC, see refs. [7] and [8,9], respectively). In particular, in a BFC, the redox polymer matrix provides a highly solvated environment due to its hydrogel properties. At the same time it ensures electrical wiring of the redox active biocatalyst by mediated electron transfer (MET).[1–3] In a BSC, the redox polymer acts simultaneously as a pseudo-capacitive element and hence as the charge storing matrix, which is oxidized/reduced by the proceeding enzymatic reaction under turnover conditions and at open circuit.[5] The driving force for this self-charging process is due to the potential difference between the redox active biocatalyst and the used pseudo-capacitive element.[5] In some cases also light can be used as a trigger for this process.[10]

The conventional design of a BFC involves the use of a redox polymer with a mid-point redox potential (E) that is close to the redox potential of the biocatalyst to ensure a minimum overpotential to drive the enzymatic reaction and thus minimizing losses in OCV (Figure 1a).[1–3,11] However, in this configuration the device is a poor BSC due to the low driving force that is provided to change the *ox-to-red* ratio in the pseudo-capacitive element.[12,13] Consequently, according to the Nernst equation (eq. 1) only a slight Nernst-shift that depends on the ratio a_{ox}/a_{red} provided no parasitic discharge by leakage currents will occur.[12]

$$E = E^0 + RT/nF \ln(a_{ox}/a_{red}) \qquad (1)$$

(where a_{ox} and a_{red} are the activity of the oxidized, and the reduced species, respectively; E^0 = formal potential and R, T, n and F have their usually meaning). In the capacitor mode the gap between the redox potentials of the redox polymer and the enzyme must be large to ensure an effective charging of the polymer as it was demonstrated for the first intrinsic BSC in which $E_{anode} > E_{cathode}$ in the non-charged state and $E_{anode} <$

[a] Dr. S. Alsaoub, Dr. F. Conzuelo, Prof. Dr. W. Schuhmann, Dr. A. Ruff
Analytical Chemistry – Center for Electrochemical Sciences (CES)
Faculty of Chemistry and Biochemistry, Ruhr University Bochum
Universitätsstr. 150, D-44780 Bochum, Germany.
E-mail: wolfgang.schuhmann@rub.de; adrian.ruff@rub.de
[b] Dr. N. Mano, S. Gounel
University of Bordeaux, CRPP, UMR 5031 33600 Pessac, France
[c] Dr. N. Mano, S. Gounel
CNRS, CRPP, UMR 5031, 33600 Pessac, France.

Supporting information for this article is given via a link at the end of the document.

$E_{cathode}$ in the charged state (Figure 1b).[13] In this configuration, a BFC would not produce an effective OCV and, thus, this device can only act as a BSC. However, recently, we demonstrated that this Nernstian shift does not only occur in BSC devices but also affects the potential of pseudo-capacitive electrodes in BFCs, provided that $E_{mediator}$ significantly differs from $E_{biocatalyst}$.[11] Consequently, the observed OCV of a BFC equipped with a polymer/glucose oxidase (GOx) based bioanode operating in a MET regime (pseudo-capacitive electrode) and bilirubin oxidase (BOx) based biocathode operating in a direct electron transfer (DET) regime was effectively larger (500 mV) than the expected value (300 mV) determined as the potential difference between redox mediator at the bioanode (≈+200 mV vs. Ag/AgCl/3 M KCl) and the visible onset for O_2 reduction at the biocathode (≈+500 mV vs. Ag/AgCl/3 M KCl).[11] A similar effect was observed when the same redox polymer was used at the bioanode and biocathode (effective OCV of ≈400 mV).[9,11] Evidently, in both cases, i.e. in BFC and in BSC mode, the performance of the device will be affected by the degree of the shift of the redox potential in the pseudo-capacitive elements.[14,15] Thus, a combination of both systems in a hybrid device solely based on pseudo-capacitive polymer/enzyme electrodes should be possible and should ensure high operating voltages in energy conversion (BFC) as well as in energy storage (BSC) mode by using redox polymers with adapted potentials[14], that is, potentials that significantly differ from the potentials of the corresponding enzyme but still ensure a substantial voltage difference in a classical fuel cell scheme (Figure 1c). We want to emphasize that in any of these three cases the OCV will always be below the theoretical thermodynamic limit that is based on the potentials of the fuel/oxidant since the catalyst itself requires a certain overpotential (η in Figure 1) to drive the oxidation/reduction of the fuel/oxidant. Consequently, in a catalytic reaction the potential difference between (bio)catalysts used at anode and cathode reflects the intrinsic limit of the OCV for the assembled (bio-)fuel cell.

Here, we report the fabrication of a BFC/BSC hybrid device fully based on redox polymer/enzyme electrodes, providing a pronounced OCV in both operating modes by adapting the redox potentials of the pseudo-capacitive elements, i.e. the redox polymers used for the bioanode and the biocathode, by careful selection of appropriate mediator species with fine-tuned potentials.

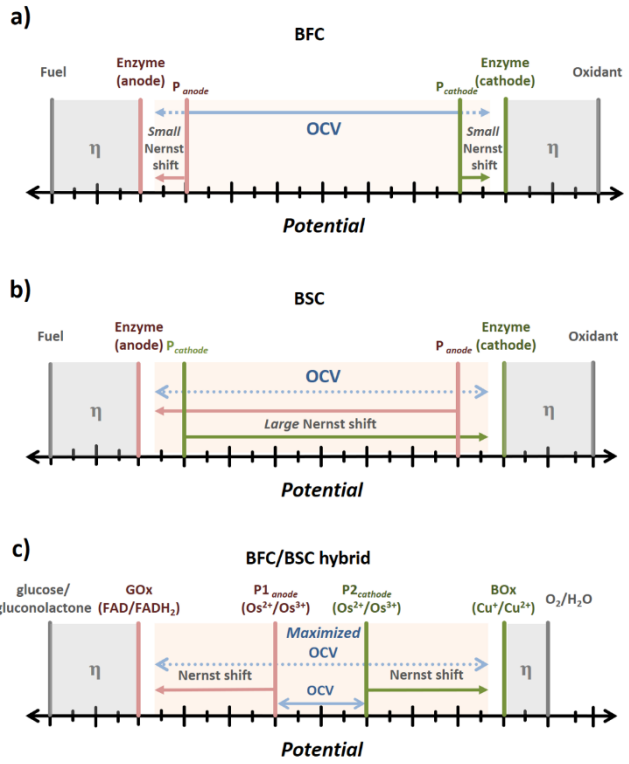

Figure 1. Schematic illustration of the redox potentials involved in a classical BFC (a), in an intrinsic BSC (b) and in the proposed BFC/BSC hybrid device (c). P_{anode} and $P_{cathode}$ indicate the redox potentials of the redox polymers used for wiring of the anodic and cathodic biocatalyst; η indicates the overpotential that the catalyst requires to convert the fuel/oxidant that are ≈300 mV for GOx/glucose and ≈130 mV for BOx/O_2. The gap between the potentials of the fuel and oxidant represents the thermodynamic limit of the OCV for the corresponding system. Blue arrows indicate the resulting OCV; red and green arrows indicate the Nernst shift under turnover conditions that is induced by the enzyme driven self-charging process of the pseudo-capacitive elements, i.e. the redox polymers. As biocatalysts for the hybrid device glucose oxidase (GOx) and bilirubin oxidase (BOx) were employed. **$P1_{anode}$** and **$P2_{cathdoe}$** represent the low and high potential polymer poly(1-vinylimidazole-*co*-allylamine)-[Os(dmxybpy)$_2$Cl]$^{2+}$ and poly(1-vinylimidazole-*co*-[2-(methacryloyloxy)ethyl]trimethylammonium chloride)-[Os(bpy)$_2$Cl]$^{+}$, respectively. FAD/$FADH_2$ = flavin adenine dinucleotide redox couple. Cu^{+}/Cu^{2+} = redox couple in the T1 cluster in BOx. Potential shifts are not drawn to scale.

Results and Discussion

BFC-BSC hybrid device - Concept

To ensure the operational functionality of a hybrid device, a careful selection of the redox polymers for a given set of biocatalysts for the anodic (conversion of fuel) and the cathodic (conversion of the oxidant) reaction has to be made: (i) to ensure a high driving force to induce an effective Nernst-shift and by this to establish a high OCV in a BSC device the potential difference

between the biocatalyst and the corresponding redox polymer matrix has to be large and (ii), the potential gap between the redox polymer for the anode an the cathode has to be significant to ensure a considerably large OCV in the BFC mode that can be further enhanced during turnover by inducing a Nernstian shift in a corresponding pseudo-capacitive electrode[11] (Figure 1c). Evidently, a careful adaption of the potential of the immobilization matrices is prerequisite for a pronounced performance of the device in terms of maximized OCV values.

As biocatalysts for the bioanode and biocathode we selected the robust and highly active enzymes GOx from *Aspergillus niger* (commercial source) and BOx from *Bacillus pumilus*[16], respectively. The potential of the FAD unit in GOx is located at around ≈ -300 mV vs. Ag/AgCl/3 M KCl [17] that is around 300 mV more positive than the thermodynamic potential of the redox couple glucose/glucono-1,5-lactone (≈ -600 mV vs. Ag/AgCl/3 M KCl, [18,19] thermodynamic anode potential). The redox potential of BOx at pH 7 is expected to be at around ≈ +450 mV vs. Ag/AgCl/3 M KCl [16,20] and thus ≈130 mV more negative than the O_2/H_2O couple (+580 mV vs. Ag/AgCl/3 M KCl,[18,19] thermodynamic cathode potential). Assuming an effective Nernstian shift during charging under turnover of around Δ = 200 mV,[11,12] redox polymers with potentials of ≈ 0 mV (bioanode) and ≈+200 mV (biocathode) are desired. This would lead to a theoretical OCV of the BFC of around 200 mV neglecting charging effects. In the following, the low and high potential polymers will be designated as **P1** and **P2**, respectively.

Synthesis of redox polymers: P1 and P2

Os-complex modified polymers were used as electron relays for various enzymes and also proved to be suitable to act as charge storing matrix in BSCs.[9,12,13] Moreover, a rational ligand design for the polymer bound Os-complexes allows fine tuning of the redox potential, e.g. by introduction of electron-withdrawing (shift to more positive potentials) or electron-donating groups (shift to more negative potentials) into the ligand sphere.[21]

For the synthesis of the low potential polymer **P1** we used the Os-complex precursor $[Os(dmxy\text{-}bpy)_2Cl_2]Cl$ which was synthesized by replacing four of the Cl-ligands in $[Os(IV)Cl_6]^{2-}$ with two bidentate dimethoxy-substituted bipyridine (dmxy-bpy) ligands in ethylene glycol at elevated temperatures (Scheme 1a).[22] During synthesis, the solvent ethylene glycol acts as reducing agent and ensures the formation of the Os(III)-species[23] (note that due to the low redox potential the Os-complex cannot be isolated as the Os(II) species under the given conditions and reduction stops at Os(III) species). The two electron-donating dimethoxy-groups at the bpy-core ensure a low potential of the Os(III)-complex (*E* ≈ -270 mV vs. Ag/ AgCl/3 M KCl, Figure S1a). Complexation of $[Os(dmxy\text{-}bpy)_2Cl_2]Cl$ to poly(1-vinylimidazole-*co*-allylamine) (P(VI-AA)) in refluxing methanol gave rise to the low potential polymer poly(1-vinylimidazole-co-allyamine)-$[Os(dmxy\text{-}bpy)_2Cl]^{2+}$, **P1** (Scheme 1b) that reveals a redox potential of -40 mV vs. Ag/ AgCl 3 M KCl) (Figure S1d), which is close to the desired value of 0 V. The use of a rather moderate temperature for the synthesis of this polymer seems to be of particular importance. Analogous reactions in refluxing ethanol (higher boiling point than methanol) showed the formation of undefined side products evidenced by an additional peak at more positive potentials in cyclic voltammograms measured with drop cast films. However, the complexation rate was much lower at these temperatures and an extensive work up (size exclusion chromatography using a Sephadex column) to remove the remaining $[Os(dmxy\text{-}bpy)_2Cl_2]^+$ was required.

The positively charged polymer should enhance interactions with the predominantly negatively charged surface of GOx.[24] Moreover, the primary amino groups in **P1** (and also amino surface groups in GOx) can be reacted with the bifunctional crosslinker poly(ethylene glycol) diglycidyl ether (PEGDGE) to ensure stable polymer/enzyme composite films.

For the high potential polymer **P2**, the Os-complex precursor $Os(II)(bpy)_2Cl_2$, that contains two bidentate bpy-cores (introduced in ethylene glycol at elevated temperatures, Scheme 1a), was bound to poly(1-vinylimidazole-*co*-[2-(methacryloyloxy)ethyl] trimethylammonium chloride)) (**P(VI-MADQUAT)**) in refluxing ethanol via a ligand exchange reaction (Scheme 1c). The absence of electron donating groups at the bpy-cores in $Os(II)(bpy)_2Cl_2$ ensure the formation of a high potential Os(II)-complex precursor (*E* = +30 mV vs. Ag/AgCl/3 M KCl, Figure S1b). The potential of the polymer bound complex is further shifted to more positive values due to the replacement of one Cl-ligand (strong electron-donor) by an imidazole unit of the backbone to +190 mV vs. Ag/AgCl/3 M KCl (Figure S1e). Again, this value is close to the envisaged redox potential of +200 mV. In analogy to the **P1**/GOx system, the positively charged polymer **P2** should facilitate an intimate contact with the predominantly negatively charged BOx surface.

We want to emphasize that all results obtained from the electrochemical (Figure S1) and UV-vis spectroscopic (Figure S2) cha-

racterization of the free Os-complex precursors [Os(III)(dmxy-bpy)$_2$Cl$_2$]Cl and Os(II)(bpy)$_2$Cl$_2$ as well as of the redox polymers **P1** and **P2** are consistent with the proposed molecular structures depicted in Scheme 1.

P1/GOx- and P2/BOx-based bioelectrodes

The biocatalytic activities of the drop cast redox polymer/enzyme films **P1**/GOx and **P2**/BOx on graphite electrodes and cross-linked with PEGDGE were investigated by means of cyclic voltammetry in phosphate buffer (PB) at pH 7.3 (Figure 2) in absence (black traces) and the presence of substrate (red traces). The half-wave potential of the anodic and cathodic catalytic wave matches nicely the redox potential of **P1** (Figure 2a) and **P2** (Figure 2b), respectively. Hence, we conclude that the redox proteins are wired via a MET regime to the electrode surface (note that in contrast to the pristine polymer film measured in aqueous KCl and on glassy carbon electrodes the potentials of the redox polymers on graphite electrodes and in combination with the enzyme, crosslinker and in PB were slightly shifted to more positive values: **P1**/GOx: 0 mV, **P2**/BOx: +200 mV).

The pronounced catalytic response under turnover conditions (maximum absolute current densities J: **P1**/GOx: $J \approx 65$ µA cm^{-2}; **P2**/BOx: $J \approx 150$ µA cm^{-2}; red traces in Figure 2) confirm good interactions between the biocatalysts and the specifically designed polymers. Moreover, it can be anticipated that also the high thermodynamic driving force based on the large potential difference between the enzyme and the corresponding polymer significantly contributes to a productive MET process.

Biosupercapacitor mode – energy storage

The performance of the **P1/GOx**//**P2/BOx** hybrid device in BSC mode was investigated by analyzing the course of the potential of the individual bioelectrodes mounted in a two-compartment cell in the presence and absence of the substrates (Figure 3a). Both electrodes show a rather steep shift in potentials upon the addition of O_2 (air purge, biocathode, red trace, t = 110 s) and 0.1 M glucose (bioanode, black trace, t = 660 s) indicating a fast charging of the pseudo-capacitive element by the enzymatic reaction, i.e. the transformation of Os(III) species at the bioanode into Os(II) moieties and transformation of Os(II) species at the biocathode to Os(III) moieties. This fast charging process is achieved because of fast enzyme kinetics and sufficient mass transport of the substrate towards the electrode and is driven by a substantial potential difference between the midpoint potential of the redox polymer and the redox potential of the enzyme that ensures a high driving force.

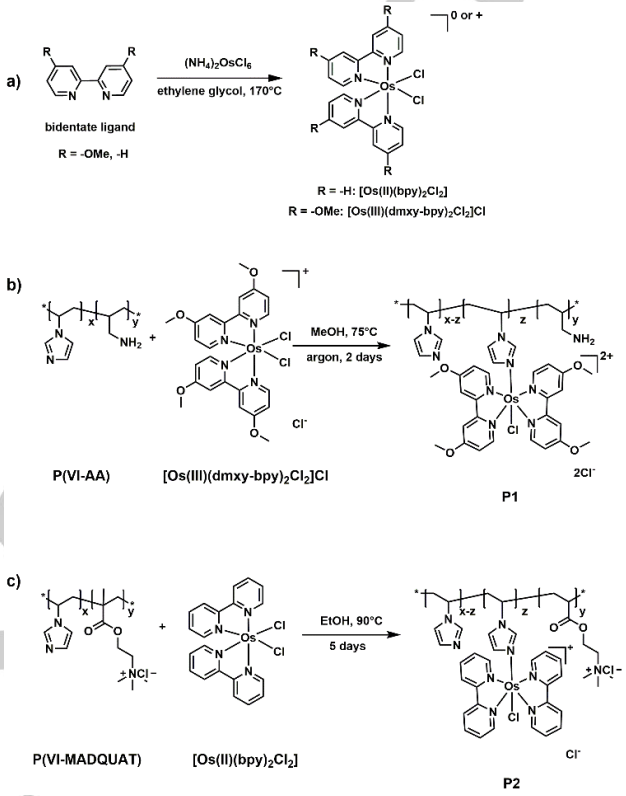

Scheme 1. Synthesis of the Os-complex precursors [Os(III)(dmxy-bpy)$_2$Cl$_2$]Cl (R = -OMe) and Os(II)(bpy)$_2$Cl$_2$ (R = -H) (**a**) and the low (**b**) and high (**c**) potential polymer **P1** (poly(1-vinylimidazole-*co*-allylamine))-[Os(dmxy-bpy)$_2$Cl]$^{2+}$) and **P2** (poly(1-vinylimidazole-*co*-[2-(methacryloyloxy)-ethyl]trimethylammonium chloride)-[Os(bpy)$_2$Cl]$^{+}$). The Os-complex precursors (**a**) were synthesized by reacting two equivalents of the corresponding bidentate ligand with one equivalent of $(NH_4)_2OsCl_6$ in hot ethylene glycol. Attachment of the complexes to the polymer backbone was achieved in refluxing methanol (**P1**, **b**) or ethanol (**P2**, **c**) by substituting one of the chloro ligands in the precursor with a single imidazole unit within the polymer backbone. The lower boiling point of methanol in the synthesis of **P1** avoids the formation of an undesired electroactive by-product that was formed at higher temperature.

The slight drift in OCP before substrate addition might be induced by traces of oxygen (note that prior to the OCP measurements the electrodes were polarized at the midpoint potential of the corresponding redox polymer to ensure $a_{ox}/a_{red} = 1$ at t = 0 s). In case of the biocathode, O_2 traces will invoke the enzymatic reaction and electrons are extracted from the polymer matrix by the turn-over of the enzyme with the concomitant increase in

electrode potential. The reduced low potential polymer **P1** at the bioanode is most likely re-oxidized by O_2 traces and thus the OCP is slightly increasing for t < 660 s (note that Os-complexes with E < +70 mV vs. Ag/AgCl/3 M KCl can act as catalysts for the oxygen reduction reaction[25]). Nevertheless, the change in OCP after the addition of the substrate is much more pronounced and reaches a steady state within a short time scale. Both OCP values were shifted by about Δ = 200 mV reaching ≈+420 mV vs. Ag/AgCl/3 M KCl at the biocathode and ≈-180 mV vs. Ag/AgCl/3 M KCl at the bioanode, resulting in a remarkably high OCV of 600 mV. We want to emphasize again that the potential of both electrodes only depends on the *ox-to-red* ratio of the polymer-bound redox couples within the pseudo-capacitive element. The degree of potential shift depends on the potential difference between the enzyme and the redox mediator that ensures a high driving force even in the charged state that is indeed the case for the **P1**/GOx and **P2**/BOx couples in the proposed hybrid device. However, the rate of charging depends on the enzyme kinetics and substrate mass transport. For both electrodes charging seems to be fast (within s, Figure 3b), which is crucial for a proper operation in pulse mode (BSC configuration, multiple charge/discharge cycles).

Applying a constant load of 10 kΩ at t = 1970 s leads to a fast discharge of the device and the potential values of the individual electrodes reach their initial values again. At open circuit (t = 2070 s) the charging process is visible again.

The ability to store charges over a longer period was tested by transferring the charged electrodes into substrate free electrolyte. Only a slight change of the OCP values was observed within ≈4000 s (Figure S3). Moreover, multiple charge/discharge cycles can be performed without a significant decrease of the resulting OCV and current output of the device over a period of 14 h (Figures 3b and c, Figure S4). The shape of the decay of the current spike by applying a constant load (Figure 3c) strongly suggests a diffusion controlled discharging process (diffusion of counterions in/out of the film) that follows a Cottrell-type behavior ($I \sim t^{-1/2}$). This behavior is in line with previously reported results on polymer/enzyme based BSCs.[13] The maximum current spike during a discharge cycle (absolute current value at the beginning of the discharging process) was about ≈35 µA (≈357 µA cm^{-2}).

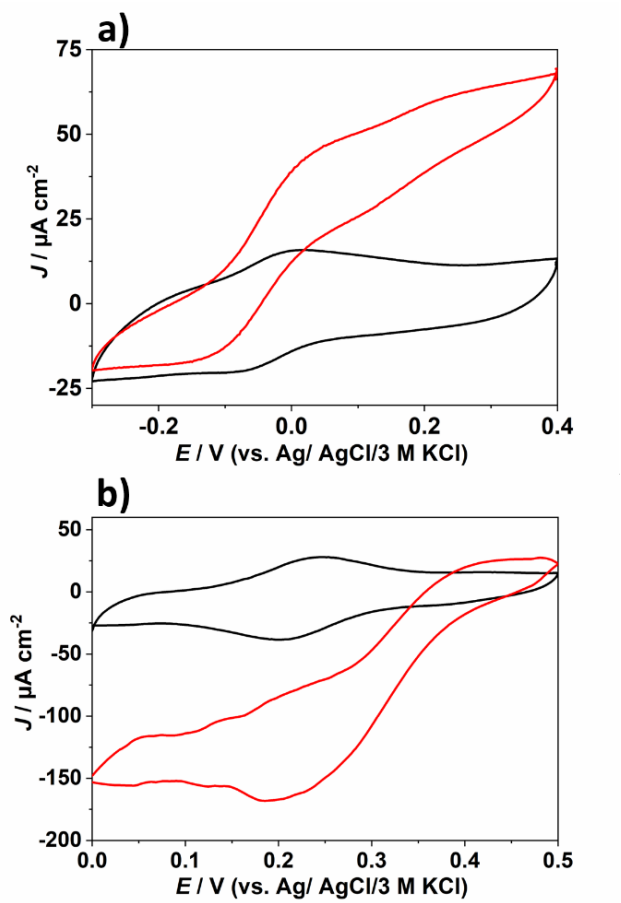

Figure 2. Cyclic voltammetric characterization in 0.1 M phosphate buffer at pH 7.3 of **P1**/GOx/PEGDGE (**a**) and **P2**/BOx/PEGDGE (**b**) films deposited on graphite electrodes (d = 6 mm) via a drop-cast process in the absence (black curves) and in the presence of substrates (red curves, **a):** 0.1 M glucose, **b):** air-purge; potential cycles were recorded at scan rates of 2 mV s^{-1} (**a**) and 5 mV s^{-1} (**b**). Specific polymer and enzyme loadings **a)**: **P1** = 536 µg cm^{-2}; GOx = 214 µg cm^{-2}; **b**) **P2** = 536 µg cm^{-2}; BOx = 580 µg cm^{-2}. The shape of the *I-E* curve at E < 0.15 V under turnover conditions in b) is attributed to mass transport fluctuations induced by air purging.

Biofuel cell mode – energy conversion

From the potential difference of the used redox relays for the bioanode (-40 mV vs. Ag/AgCl/3 M KCl) and the biocathode (+190 mV vs. Ag/AgCl/3 M KCl) a theoretical OCV of 230 mV could be expected when the hybrid device is operated in biofuel cell mode. However, under operation conditions the OCV of the **P1**/GOx//**P2**BOx-based BFC as measured in a two-compartment configuration was (580 ± 40) mV (determined from three independent experiments) that is considerably higher than the expected value but of course lower than the thermodynamic limit (≈1.18 V) given by the potential difference of the fuel (glucose/gluconolactone) and oxidant (O_2/H_2O).[18,26] Moreover, the

value is consistent with the value obtained for the BSC (Figure 3a). Thus, we conclude that the Nernstian-shift that occurs for both electrodes indeed enhances the experimental OCV value even in BFC mode.

The maximum power density (*P*) and maximum *J*-values were derived to be (7 ± 3) µW cm^{-2} at 250 mV and (43 ± 9) µA cm^{-2}, respectively (values were calculated from 3 independent measurements, Figure 4a). The operational stability in BFC mode was evaluated by applying a constant voltage of +250 mV between the bioelectrodes corresponding to the voltage at which the maximum power output was obtained. After an initial current drop, most likely due to loss of charges accumulated under turnover at open circuit, the current output remains rather stable (Figure 4b). Only a slight decrease from ≈20 µA cm^{-2} to ≈16 µA cm^{-2} was observed over a period of 3.5 h.

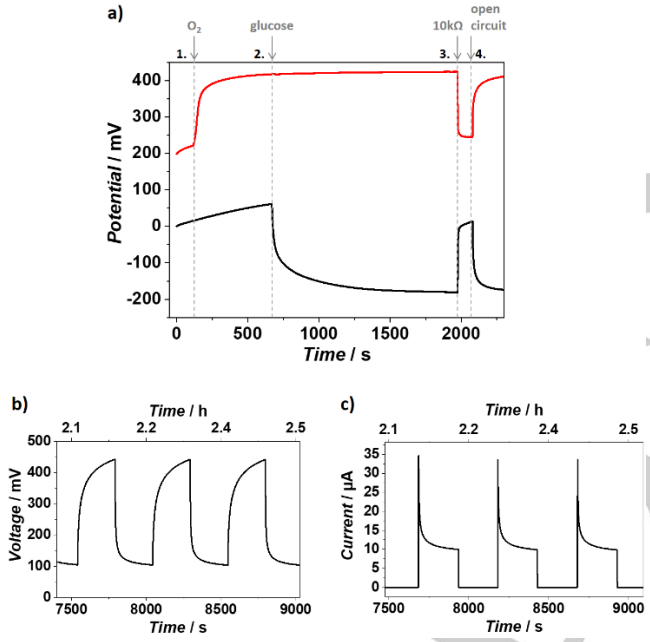

Figure 3. Characterization of the BSC of the hybrid device in a two-compartment configuration. **a**) Course of the potentials of the **P1**/GOx/PEGDGE (black line) and **P2**/BOx/PEGDGE (red line) electrodes during the self-charging process (t < 1970 s) and during discharge/charge process (t > 1970 s). The pseudo-capacitive electrodes were first charged by adding the corresponding substrate: bioanode compartment: glucose (0.1 M), t = 660 s; biocathode compartment: O_2 (air purge), t = 110 s. The capacitor was discharged at a constant load of 10 kΩ at t = 1970 s. When removing the load (t = 2070 s) the self-charging process is again observed. Voltage (**b**) and current (**c**) response during multiple charge/discharge cycles. Discharge was conducted at a constant load of 10 kΩ. Specific polymer and enzyme loadings: **P1** = 2143 µg cm^{-2}; GOx = 214 µg cm^{-2}; **P2** = 536 µg cm^{-2}; BOx = 580 µg cm^{-2}. Working electrolyte: 0.1 M PB, pH 7.3. Anode compartment was argon flushed.

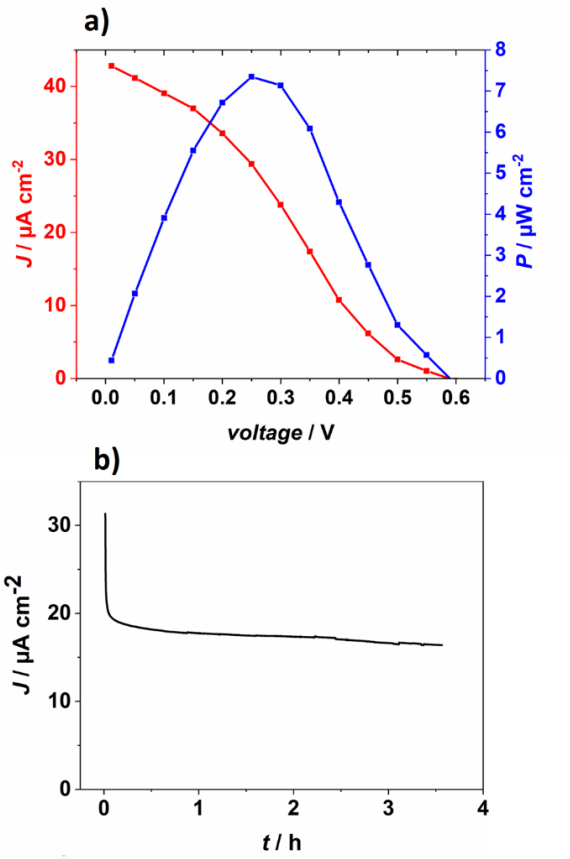

Figure 4. Characterization of the BFC performance of the hybrid device. **a)** Average power density (*P*, blue) and current density (*J*, red) values as a function of applied voltage (from 3 independent experiments). Maximum power density ≈7.3 µW cm^{-2} was reached at 250 mV; lines are guidance for eyes only. **b**) Operational stability at an applied voltage of 250 mV. After an initial drop the current remains rather stable within the time scale of the experiment indicating the good stability of the polymer/enzyme electrodes in the hybrid device. Experiments were conducted in a two-compartment cell; working electrolyte: 0.1 M PB, pH 7.3; anode compartment: argon atmosphere, 0.1 M glucose; cathode compartment: air saturated buffer. Specific polymer and enzyme loadings: **P1** = 2143 µg cm^{-2}; GOx = 214 µg cm^{-2}; **P2** = 536 µg cm^{-2}; BOx = 580 µg cm^{-2}.

For comparative purposes and to demonstrate the effect of the Nernstian shift on the OCV value, we constructed a BFC based on an O_2-insensitive pyrroloquinoline quinone-dependent glucose dehydrogenase (PQQ-GDH, bioanode) and again a BOx (biocathode) that were wired via the redox polymers **P1** (Figure S5a) and the high potential polymer **P3** (Figure S5b), i.e. poly(1-vinylimidazole-*co*-allyamine)-[Os(diCl-bpy)$_2$Cl)]$^+$ (Scheme S1), respectively. **P3** bears a high potential Os-complex that is equipped with Cl-substituted bpy ligands that ensure a strong electron withdrawing effect on the Os-center and thus a high redox potential for the Os-complex precursor Os(diCl-bpy)$_2$Cl$_2$ (E =

+170 mV vs. Ag/AgCl/3 M KCl, Figure S1c). Attachment of this Os-complex precursor to the P(VI-AA) backbone, leads to the high potential redox polymer **P3** that reveals a redox potential of *E* = +420 mV vs. Ag/AgCl/3 M KCl (Figure S1f). This value is close to the value of the cathodic biocatalyst BOx (≈+450 mV vs. Ag/AgCl/3 M KCl at pH 7). Thus, we expect only little charging due to a reduced thermodynamic driving force for the self-charging process at the biocathode. In addition, the PQQ co-factor in PQQ-GDH shows a redox potential of around ≈ -150 mV vs. Ag/AgCl/3 M KCl [27] that is close to the redox potential of polymer **P1** (-40 mV vs. Ag/AgCl/3 M KCl). Hence, the charging at the bioanode is also hampered by a lower driving force. Consequently, in this rather classical fuel cell design the experimental OCV value should be closer to the theoretical value of 460 mV with only a minor contribution of charging. Indeed, the OCV value measured under operational conditions in a one-compartment cell (note that in this case the Ohmic losses should be much smaller compared to the two-compartment cell and should even further enhance the OCV value compared to the two-compartment system) was (600 ± 10) mV. Evidently, also in the **P1**/PQQ-GDH//**P3**/BOx system a Nernstian-shift is contributing to an enhanced OCV value, however it is significantly less pronounced (enhancement by 140 mV, which is almost the maximum considering the redox potentials of the used enzymes which reflects an intrinsic limit for the charging process) compared to the **P1**/GOx//**P2**/BOx based hybrid device (enhancement by 470 mV, shift of Δ = ± 200 mV in both directions, see also Figure 3a). Evidently, for a good performing hybrid device the selection of the biocatalyst and/or polymer to ensure enough potential difference between the enzyme and the redox relay is of particular importance.

The voltage at that the maximum power density ((4 ± 1) μW cm^{-2} at) in the **P1**/PQQ-GDH//**P3**/BOx BFC was reached was estimated to be 300 mV (see Figure S6 for a representative power curve). This value is only somewhat higher than the one of the hybrid device (250 mV). Thus, our results nicely show that it is indeed possible to build a BSC/BFC hybrid device providing an efficient performance and with an optimized OCV.

The lower power density of the classical BFC assembly is attributed to the poorly performing **P3**/BOx biocathode (Figure S5b), that shows substantial lower currents than the **P2**/BOx biocathode (Figure 2b), most likely due to a reduced thermodynamic driving force based on the small potential gap between **P3** and BOx.

Conclusions

The proposed concept provides access to a BFC/BSC hybrid device with optimized operational voltage in both operating modes. The hybrid system was equipped with pseudo-capacitive elements, i.e. redox polymers with adapted potentials, at the bioanode and biocathode that ensured a significant Nernstian-shift at both electrodes under turnover conditions and thus ensured a maximized OCV of the device. Our results clearly demonstrate that the rational design of the electron relay matrix and the careful selection of the biocatalyst leads to biodevices with multifunctional properties that can be used as energy conversion or energy storage device on demand. Moreover, the performance of the hybrid device in BFC mode is similar to the properties measured with a rather classical fuel cell design.

It can be anticipated that the proposed concept opens new design strategies for the fabrication of high performance bioelectrochemical systems that might be not accessible by following conventional approaches. This might include the design of suitable polymer matrixes that ensure higher film stability by introduction of highly efficient/reactive crosslinking capabilities or the additional functionalities by the incorporation of specific functional groups (e.g. thermo- or pH-responsive groups) to the polymer backbone which would otherwise not be possible or strongly hampered if one is limited to a certain type of mediator with a fixed potential. Moreover, by further controlling the density of redox sites within the pseudocapacitive elements, i.e. number of redox centers attached to the polymer backbone, by a controlled and carefully conducted synthesis, not only the operational voltage but also the current output as well as the capacitance of such hybrid devices can be controlled in a straightforward way.

Experimental Section

Materials and Methods

All chemicals, materials and solvents were purchased from Sigma-Aldrich, Merck, TCI, Alfa-Aesar, Acros Organics, VWR and J.T. Baker and were used as received except otherwise noted. Deuterated solvents were purchased from Deutero and Euriso-top and were stored at 4 °C (DMSO-d_6 was stored at room temperature). The aqueous solutions were prepared by using deionized water that was prepared with a Milli-Q system from Millipore.

NMR experiments were conducted at room temperature with a Bruker DPX-200 spectrometer with a ^{1}H resonance frequency of 200.13 MHz or with a DPX-400 spectrometer with a ^{1}H resonance frequency of 400.13 MHz. Chemical shifts were referenced to the residual solvent peak and

are reported in ppm. UV-Vis absorption measurements were recorded using a 60 UV-Vis spectrophotometer from Agilent Technology using quartz cuvettes with an optical path length of 1 cm.

Redox polymers

The polymer backbone poly(1-vinylimidazole-*co*-allylamine) P(VI-AA) and the Os-complex precursor $Os(bpy)_2Cl_2$ were prepared following procedures described in [11]. The polymer backbone poly(1-vinylimidazole-*co*-[2-(methacryloyloxy)ethyl]trimethylammonium chloride) P(VI-MADQUAT) was synthesized according to previously described procedures [13]. The detailed synthesis and characterizations of $[Os(III)(dmxy\text{-}bpy)_2Cl_2]Cl$, $Os(II)(diCl\text{-}bpy)_2Cl_2$, **P1**, **P2** and **P3** can be found in the Supporting Information.

Enzymes

Glucose oxidase (GOx) from *Aspergillus niger* (type X-S, lyophilized powder, 100,000–250,000 units g^{-1}) was purchased from Sigma–Aldrich and stored at -20 °C. The enzyme solution was prepared in a concentration of 20 mg ml^{-1} in phosphate buffer (pH 7.3). Bilirubin oxidase (BOx) from *Bacillus pumilus* in 50 mM borate buffer (pH 9) with a protein concentration of 54.75 mg mL^{-1} (determined in 1 mM 2,2'-azino-bis(3-ethylbenzothiazoline-6-sulphonic acid (ABTS) in 50 mM citrate/phosphate buffer, pH 4) and an activity of 713 units mg^{-1} was obtained as recently described.[28] The apo enzyme of pyrroloquinoline quinone-dependent glucose dehydrogenase (PQQ-GDH) form *Acinetobacter calcoaceticus* (Mut-Q-GDH_2 mutant of the native GDH) was a gift from Roche Diagnostics, Penzberg/Germany. Reconstitution was conducted as follows: to a PQQ solution (520 µM) in HEPES buffer (80 µL, 10 mM, pH 7.0) $CaCl_2$ was added (1.76 mg, 150 mM) followed by the addition of the solid GDH (2.16 mg). Reconstitution was completed after 30 minutes at room temperature in the dark. The PQQ-GDH solution was stored at 4 °C in the dark. The concentration of the PQQ-GDH was estimated to be 25 mg mL^{-1} assuming a quantitative complexation of PQQ to the protein.

Preparation of the polymer/enzyme electrodes

The bioelectrodes were prepared by drop casting the corresponding polymer, enzyme and poly(ethylene glycol) diglycidyl ether (PEGDGE, crosslinker) mixtures (mixed with a Vortex mixer) onto graphite electrodes with a nominal diameter of 6 mm (A = 0.28 cm^2). The electrodes were dried for several hours at room temperature or at 4 °C.

Bioanodes. For the **P1**/GOx/PEGDGE bioanode **P1** (60 mg mL^{-1} in water), GOx (20 mg mL^{-1} in PB, pH 7.3) and PEGDGE (0.0114 mg mL^{-1} in water) were mixed in a volumetric ratio of 10:3:2 and drop cast onto the graphite working electrodes. For the **P1**/PQQ-GDH bioanodes **P1** (38 mg mL^{-1} in water) and PQQ-GDH (25 mg mL^{-1} in HEPES buffer) were mixed in a volumetric ratio of 2:1 and drop cast onto the electrode surface.

Biocathodes. For the preparation of the **P2**/BOx/PEGDGE biocathodes the polymer **P2** (15 mg mL^{-1} in water), BOx (54.75 mg mL^{-1}) and PEGDGE (0.0114 mg mL^{-1} in water) were mixed in a volumetric ratio of 10:3:2 and drop cast onto graphite electrodes. The **P3**/BOx biocathodes were prepared by mixing **P3** (7 mg mL^{-1} in water) and BOx (54.75 mg ml^{-1}) in a volumetric ratio of 10:1 and drop cast onto the electrode surface.

Electrochemical measurements

Cyclic voltammetric experiments were performed at room temperature with an Autolab FRA2 µAutolab Type III potentiostat from Metrohm in a one-compartment three-electrode cell under argon or ambient atmosphere (see text). A Pt wire with 1 mm diameter was used as the counter electrode. For the reference electrode an Ag/ AgCl/3 M KCl system was employed. As working electrodes, graphite electrodes (GEs) with diameters of 6 mm (geometrical surface area A = 0.28 cm^2) or glassy carbon electrodes with a nominal diameter of 3 mm (A= 0.07 cm^2) were used. As electrolyte solutions either aqueous KCl solution or phosphate buffer (pH 7.3) were used. Depending on the experiment, the electrolyte was purged with the corresponding gas to ensure saturation concentrations. The capacitor tests were conducted in a two-compartment cell separated by a Nafion membrane with a two-electrode setup. Pre-conditioning of the redox polymers was done in a four-electrode configuration in the same cell. The measurements were carried out with a bi-potentiostat (PGU-BI 100, IPS-Jaissle Electronik). The capacitor-setup was described in detail in [12]. Biofuel cell measurements were carried out in a two-electrode configuration in a one or a two-compartment cell. The BFC measurements were recorded following a procedure reported in [29]. The power curve of the BFC was obtained by applying potential pulses starting from the measured OCV. Steady state currents were used for the calculation of the power curve. All BSC and BFC measurements were performed at room temperature in 0.1 M phosphate buffer at pH 7.3. The open circuit values were determined from the extrapolation of the power curve at y = 0.

Acknowledgements

The authors thank Melinda Nolten and Jana Becker for the help with the synthesis of some of the precursors and the Os-complexes and for performing some of the electrochemical experiments. This work was supported by the Deutsche Forchungsgemeinschaft (DFG, German Research Foundation) under Germany´s Excellence Strategy – EXC-2033 – project number 390677874 and by the European Commission in the framework of the ITN "ImplantSens" (Grant agreement ID: 813006). N.M. thanks the funding of the ANR project BIO3 (ANR-16-CE19-0001-03).

Keywords: biofuel cell • biosupercapacitor • redox polymers • Nernst shift • enzyme electrodes

[1] R. A. S. Luz, A. R. Pereira, J. C. P. de Souza, F. C. P. F. Sales, F. N. Crespilho, *ChemElectroChem* **2014**, *1*(11), 1751–1777.

[2] D. Leech, P. Kavanagh, W. Schuhmann, *Electrochim. Acta* **2012**, *84*, 223–234.

[3] S. D. Minteer, B. Y. Liaw, M. J. Cooney, *Curr. Opin. Biotechnol.* **2007**, *18*(3), 228–234.

[4] a) D. Pankratov, F. Shen, R. Ortiz, M. D. Toscano, E. Thormann, J. Zhang, Lo Gorton, Q. Chi, *Chem. Commun.* **2018**, *54*(83), 11801–11804; b) S. Makino, T. Ban, W. Sugimoto, *J. Electrochem. Soc.* **2015**, *162*(5), A5001-A5006; c) N. S. Malvankar, T. Mester, M. T. Tuominen, D. R. Lovley, *Chem. Eur. J.* **2012**, *13*(2), 463–468;

[5] S. Shleev, E. González-Arribas, M. Falk, *Curr. Opin. Electrochem.* **2017**, *5*(1), 226–233.

[6] a) A. Heller, *Curr. Opin. Chem. Biol.* **2006**, *10*(6), 664–672; b) A. Ruff, *Curr. Opin. Electrochem.* **2017**, *5*(1), 66–73;

[7] a) M. Cadet, S. Gounel, C. Stines-Chaumeil, X. Brilland, J. Rouhana, F. Louerat, N. Mano, *Biosens. Bioelectron.* **2016**, *83*, 60–67; b) A. G. Mark, E. Suraniti, J. Roche, H. Richter, A. Kuhn, N. Mano, P. Fischer, *Lab on a chip* **2017**, *17*(10), 1761–1768;

[8] a) K. L. Knoche, D. P. Hickey, R. D. Milton, C. L. Curchoe, S. D. Minteer, *ACS Energy Lett.* **2016**, *1*(2), 380–385; b) H. Yu, J. Wu, L. Fan, Y. Lin, K. Xu, Z. Tang, C. Cheng, S. Tang, J. Lin, M. Huang, Z. Lan, *J. Power Sources* **2012**, *198*, 402–407;

[9] X. Xiao, P. Ó. Conghaile, D. Leech, R. Ludwig, E. Magner, *Biosens. Bioelectron.* **2017**, *90*, 96–102.

[10] E. González-Arribas, O. Aleksejeva, T. Bobrowski, M. D. Toscano, Lo Gorton, W. Schuhmann, S. Shleev, *Electrochem. Commun.* **2017**, *74*, 9–13.

[11] F. Conzuelo, N. Marković, A. Ruff, W. Schuhmann, *Angew. Chem. Int. Ed.* **2018**, *57*(41), 13681–13685.

[12] D. Pankratov, F. Conzuelo, P. Pinyou, S. Alsaoub, W. Schuhmann, S. Shleev, *Angew. Chem. Int. Ed.* **2016**, *55*(49), 15434–15438.

[13] S. Alsaoub, A. Ruff, F. Conzuelo, E. Ventosa, R. Ludwig, S. Shleev, W. Schuhmann, *ChemPlusChem* **2017**, *82*(4), 576–583.

[14] D. Pankratov, Z. Blum, S. Shleev, *ChemElectroChem* **2014**, *1*(11), 1798–1807.

[15] a) D. Pankratov, P. Falkman, Z. Blum, S. Shleev, *Energy Environ. Sci.* **2014**, *7*(3), 989; b) C. Agnès, M. Holzinger, A. Le Goff, B. Reuillard, K. Elouarzaki, S. Tingry, S. Cosnier, *Energy Environ. Sci.* **2014**, *7*(6), 1884–1888;

[16] F. Durand, C. H. Kjaergaard, E. Suraniti, S. Gounel, R. G. Hadt, E. I. Solomon, N. Mano, *Biosens. Bioelectron.* **2012**, *35*(1), 140–146.

[17] S. Vogt, M. Schneider, H. Schäfer-Eberwein, G. Nöll, *Anal. Chem.* **2014**, *86*(15), 7530–7535.

[18] R. A. Alberty, *Biochem. Educ.* **2000**, *28*(1), 12–17.

[19] S. Calabrese Barton, J. Gallaway, P. Atanassov, *Chem. Rev.* **2004**, *104*(10), 4867–4886.

[20] a) N. Mano, A. de Poulpiquet, *Chem. Rev.* **2018**, *118*(5), 2392–2468; b) E. Suraniti, S. Tsujimura, F. Durand, N. Mano, *Electrochem. Commun.* **2013**, *26*, 41–44;

[21] P. Pinyou, A. Ruff, S. Pöller, S. Ma, R. Ludwig, W. Schuhmann, *Chem. Eur. J.* **2016**, *22*(15), 5319–5326.

[22] M. N. Zafar, X. Wang, C. Sygmund, R. Ludwig, D. Leech, Lo Gorton, *Anal. Chem.* **2012**, *84*(1), 334–341.

[23] L. Della Ciana, W. J. Dressick, D. Sandrini, M. Maestri, M. Ciano, *Inorg. Chem.* **1990**, *29*(15), 2792–2798.

[24] M. V. Pishko, I. Katakis, S.-E. Lindquist, L. Ye, B. A. Gregg, A. Heller, *Angew. Chem. Int. Ed. Engl.* **1990**, *29*(1), 82–84.

[25] A. Prévoteau, N. Mano, *Electrochim. Acta* **2012**, *68*, 128–133.

[26] V. Soukharev, N. Mano, A. Heller, *J. Am. Chem. Soc.* **2004**, *126*(27), 8368–8369.

[27] V. Flexer, N. Mano, *Anal. Chem.* **2014**, *86*(5), 2465–2473.

[28] S. Gounel, J. Rouhana, C. Stines-Chaumeil, M. Cadet, N. Mano, *J. Biotechnol.* **2016**, *230*, 19–25.

[29] R. Haddad, W. Xia, D. A. Guschin, S. Pöller, M. Shao, J. Vivekananthan, M. Muhler, W. Schuhmann, *Electroanalysis* **2013**, *25*(1), 59–67.

Entry for the Table of Contents (Please choose one layout)

Layout 2:

FULL PAPER

A redox polymer-based biofuel cell / biosupercapacitor hybrid device is reported. Potential tuning of the redox polymers ensured maximized OCV values in both operation modes. A new design principle for the fabrication of novel redox polymer based immobilization matrixes considering effects of a Nernstian-shift in these pseudo-capacitive elements under turnover.

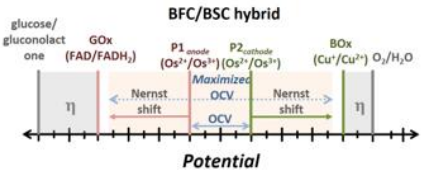

S. Alsaoub, F. Conzuelo, S. Gounel, N. Mano, W. Schuhmann, A. Ruff**

Page No. – Page No.

Introducing pseudo-capacitive bioelectrodes into a biofuel cell / biosupercapacitor hybrid device for optimized open circuit voltage